ACS EARTH AND SPACE CHEMISTRY

Article

Cite This: ACS Earth Space Chem. XXXX, XXX, XXX−XXX

http://pubs.acs.org/journal/aesccq

Production of Atmospheric Organosulfates via Mineral-Mediated Photochemistry

Mario Schmidt,[†] Shawn M. Jansen van Beek,[†] Maya Abou-Ghanem,[†] Anton O. Oliynyk,[†] Andrew J. Locock,[‡] and Sarah A. Styler*[,†]

[†]Department of Chemistry, University of Alberta, Edmonton, Alberta T6G 2G2, Canada

[‡]Department of Earth and Atmospheric Sciences, University of Alberta, Edmonton, Alberta T6G 2E3, Canada

Supporting Information

ABSTRACT: Although organosulfates ($ROSO_3^-$) comprise a significant component of secondary organic aerosol (SOA) mass, their atmospheric formation mechanisms are not fully understood. Here, using methacrolein as a model organosulfate precursor, we present a new, mineral-mediated photochemical pathway for organosulfate formation. First, we describe studies of TiO_2-catalyzed formation of the atmospherically important organosulfate hydroxyacetone sulfate from methacrolein as a function of illumination time, catalyst loading, sulfate concentration, counterion identity, and methacrolein concentration. Then, we propose a sulfate radical-mediated mechanism for organosulfate formation consistent with these observations. Finally, we show that natural Ti-containing minerals and road dust not only catalyze the formation of comparable amounts of hydroxyacetone sulfate to those formed in the presence of commercial TiO_2 but also facilitate the production of additional organosulfate species. These results highlight the complex nature of photochemistry at the surface of natural mineral samples and underscore the need for further study of the role of mineral−organic interactions in atmospheric organosulfate formation.

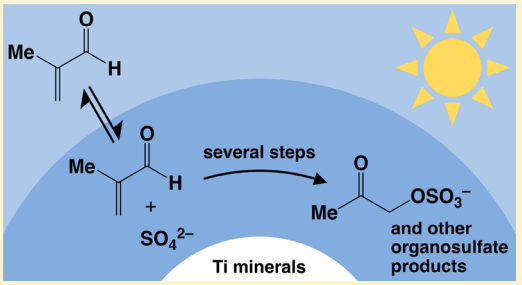

KEYWORDS: *organosulfates, photochemistry, mineral dust, road dust, methacrolein, secondary organic aerosol*

1. INTRODUCTION

Particulate matter (PM), whether emitted directly (e.g., mineral dust[1]) or formed in the atmosphere via secondary processes [e.g., secondary organic aerosol (SOA), which forms via the atmospheric oxidation of volatile organic compounds (VOCs)[2]], plays a role in many atmospheric processes. For example, PM influences Earth's climate directly by absorbing and scattering incoming solar radiation and indirectly by influencing the formation and optical properties of clouds; in addition, it contributes to reductions in air quality and human health.[3] PM also provides surfaces for chemical reactions and, thereby, influences the abundance and distribution of atmospheric trace gases (e.g., ozone and nitrogen oxides).[4]

High-resolution mass spectral analysis has revealed that heteroatom-containing compounds comprise a significant portion of the organic carbon fraction of PM.[5−9] One such class of compounds, organosulfates (OS, $ROSO_3^-$), has been measured in PM collected in a diverse range of locations, including the remote Arctic,[10] the Amazon rainforest,[11] the southern United States,[12] and urban and remote sampling sites in Asia.[13] Studies have shown that OS make a significant contribution to PM mass loadings;[14−16] for example, one large-scale study estimated that OS may make up as much as 5−10% by mass of the organic fraction of fine particulate matter ($PM_{2.5}$).[14] In addition, OS have the potential to influence PM physicochemical properties, including hygroscopicity and cloud condensation nuclei (CCN) activity.[17−19] For these reasons, the formation mechanisms of this class of compounds have been the subject of much experimental interest.

Laboratory studies have provided evidence for a wide variety of pathways for OS formation, including H_2SO_4-catalyzed esterification of alcohols,[20] nucleophilic attack by sulfate on epoxides,[21] uptake of SO_2 by long-chain alkenes and unsaturated fatty acids,[22,23] uptake of glyoxal by SO_2-aged α-Al_2O_3,[24] reaction of hydrogen sulfite with unsaturated carbonyl compounds in the presence of Fe^{3+},[25] and of particular interest to this study, the reaction of sulfate radical with organic radicals[26] and a range of unsaturated organics.[17,27−29]

In aqueous aerosol, sources of sulfate radical include the oxidation of S(IV) species in the presence of transition metal ions,[30] the hydroxyl radical oxidation of existing OS,[31] and the oxidation of hydrogen sulfate anion by the hydroxyl radical.[30] Illumination of TiO_2 with light of energy greater than its bandgap energy results in the formation of conduction-band electrons and valence-band holes, the latter of which can oxidize water to yield hydroxyl radical;[32] in addition, indirect evidence also exists for the production of sulfate radical via the

Received: November 19, 2018
Revised: January 11, 2019
Accepted: January 28, 2019

DOI: 10.1021/acsearthspacechem.8b00178
ACS Earth Space Chem. XXXX, XXX, XXX−XXX

direct, hole-mediated oxidation of sulfate at the TiO_2 surface.[33] In this context, we hypothesized that TiO_2 and Ti-containing minerals would facilitate the photochemical production of OS from unsaturated organic precursors.

In this study, we first present observations of photochemical OS formation from methacrolein (MACR)—a first-generation atmospheric oxidation product[34] of isoprene, the most abundant biogenic VOC,[35] which has been shown to be present in the atmospheric aqueous phase at concentrations much higher than those predicted by its Henry's law coefficient[36]—in aqueous suspensions of TiO_2, where we use TiO_2 as a proxy for the photochemically active portion of atmospheric mineral dust.[37] To improve our understanding of this OS formation mechanism, we measured OS production as a function of illumination time, TiO_2 loading, sulfate salt concentration and cation identity, and MACR concentration. To provide further insight into the atmospheric importance of this mechanism, we also explored OS production from MACR in the presence of three natural Ti-containing minerals (anatase, ilmenite, and mica) and urban road dust. Together, these results provide new evidence for the role of mineral–organic interactions in OS formation and highlight the value of experiments performed using natural mineral samples.

2. MATERIALS AND METHODS

2.1. Experimental Apparatus. Experiments were conducted in a custom-built photochemical reactor (~70 mL total volume; Figure S1 of the Supporting Information). Samples were illuminated using a solar simulator (SunLite, Abet Technologies), the spectral irradiance of which is presented in Figure S2 of the Supporting Information. Because the solar simulator spectrum exhibits a small tail extending to the blue of the actinic region, all experiments were performed with a 295 nm long-pass optical filter (Edmund Optics) located in the solar simulator light path. To avoid sample heating, an ultraviolet (UV) hot mirror (Edmund Optics) was also placed in the light path.

To compare the photon flux in our experiments to those in the ambient environment, we used chemical actinometry of 2-nitrobenzaldehyde (2-NB).[38] Details of these experiments are presented in the Supporting Information text and Figure S3 of the Supporting Information. The photodecay rate constant for 2-NB, j(2-NB), obtained in these experiments was $(1.89 \pm 0.02) \times 10^{-3}$ s^{-1}, which is somewhat lower than those previously reported for a variety of ambient environments.[39,40] Our results, therefore, represent a lower estimate for the mineral-catalyzed photochemical production of OS in the ambient atmosphere.

2.2. Experimental Procedure. At the beginning of each experiment, the sample of interest (i.e., TiO_2 or natural minerals) was placed in the photochemical reactor; then, a stir bar and 20 mL of an aqueous Na_2SO_4 (adjusted to pH 5 using 50 mM aqueous H_2SO_4) or $(NH_4)_2SO_4$ solution of the desired concentration was added. Finally, the reactor was closed; the sample port was equipped with a rubber septum; and MACR was added via a glass syringe through the septum into the stirred suspension. To minimize evaporation of MACR, all experiments were performed at 288 K. After 15 s of stirring under dark conditions, a t = 0 min sample was taken; then, samples were illuminated for 5–40 min. To ensure equilibration with ambient O_2 levels (i.e., $\sim 3 \times 10^{-4}$ M dissolved O_2 at 288 K[41]), samples were gently stirred for the duration of each experiment.

After illumination, samples (0.5 mL) were removed from the reactor via a syringe. To avoid injections of highly concentrated sulfate salt solutions, a methanol cleanup procedure was employed.[17] In this procedure, validation of which is described in the Supporting Information text and Figure S4 of the Supporting Information, samples were added to a 15 mL centrifuge tube containing methanol (1.25 mL) as sulfate precipitation agent and potassium propyl sulfate (10 μL; 5 mg mL^{-1} in water) as internal standard. The resultant mixture was vortexed for 30 s and centrifuged for 5 min at 3000 rpm; then, the supernatant was filtered (0.2 μm nylon filter, VWR) prior to analysis to remove any remaining sulfate precipitate and/or minerals. All reported OS concentrations and peak areas are corrected for dilution (i.e., a dilution factor of 1.75:0.5). Because the propyl sulfate signal in our samples generally varied by <3%, reported results are uncorrected.

To verify that the observed OS products arose from photochemistry rather than dark reactions and that OS observed in experiments conducted using natural mineral samples did not arise from photochemistry of mineral-associated organics, we conducted a comprehensive set of control experiments, which are described in detail in the Supporting Information text. No OS products were observed in any of these experiments.

2.3. OS Quantification and Analysis. Analysis of OS was accomplished using an Agilent 1100 high-performance liquid chromatography (HPLC) system equipped with a binary pump, autosampler, thermostated column compartment held at 40 °C, and Waters Micromass Quattro Micro triple quadrupole mass spectrometer as detector. Separation was performed using a Fisher Scientific Hypersil GOLD C18 column (Fisher Scientific, 3 μm particle size, 150 × 4.6 mm) at a flow rate of 0.4 mL min^{-1}. A gradient elution was applied, with water (0.1% formic acid) as solvent A and methanol (0.1% formic acid) as solvent B: 10% B at t = 0; 2 min linear gradient to 90% B; 2 min hold; immediate reduction to 10% B; and hold until 15 min. An injection volume of 5 μL was used for all separations.

The analysis was run in multiple reaction monitoring (MRM) mode using negative-mode electrospray ionization. In all cases, the $[M - H]^- \rightarrow m/z$ 97 transition was employed for analysis and quantification. Detailed mass spectrometric parameters are presented in Table S1 of the Supporting Information, and representative chromatograms showing OS products are presented in Figure S5 of the Supporting Information.

Hydroxyacetone sulfate (HAS, m/z 153) was quantified via comparison to an external calibration curve (Figure S6 of the Supporting Information) prepared using synthesized potassium HAS as standard. The calibration curve was obtained at the beginning of the study. To verify signal stability over time, one low and one high standard from the points on the calibration curve were measured each day. In the absence of synthesized standards, peak areas were used for semi-quantitative comparative analysis of all other OS analytes. As shown in Figure S5, chromatograms of several of these analytes exhibited multiple peaks, which suggests the existence of multiple isomers for these species. All reported peak areas consist of the sum of the areas of all detected peaks at a given m/z value.

2.4. Sample Collection, Preparation, and Characterization. The natural minerals employed in this study were obtained through Minfind (www.minfind.com). The anatase, ilmenite, and mica samples were collected in Pakistan, the

DOI: 10.1021/acsearthspacechem.8b00178
ACS Earth Space Chem. XXXX, XXX, XXX–XXX

United States, and Canada, respectively. Details regarding sample pretreatment and grinding are presented in the Supporting Information. The Edmonton road dust sample consists of winter street sweepings (i.e., material collected from city streets in spring after winter application of sand and salt for road traction/safety purposes) and was obtained from one of four City of Edmonton (Alberta, Canada) snow storage facilities, located at 17 Street (north of Whitemud Drive at approximately 52 Avenue); its <45 μm fraction was isolated using a Retsch AS200 analytical sieve shaker.

Samples were comprehensively characterized using a variety of analytical techniques, which are briefly described here; further details are presented in the Supporting Information. The Brunauer−Emmett−Teller (BET) surface areas of commercial TiO_2, anatase, and ilmenite were determined using N_2 adsorption; results are presented in Table S2 of the Supporting Information. Electron microprobe analysis was used to assess the purity of the anatase, ilmenite, and mica samples; quantitative compositional data are presented in Table S3 of the Supporting Information. The Edmonton road dust sample was examined using scanning electron microscopy (SEM) with energy-dispersive spectroscopy (EDS) analysis for elemental mapping. A sample EDS spectrum and representative elemental mapping results are shown in Figure S7 of the Supporting Information. The mineralogy of all samples was assessed via X-ray diffraction analysis, as shown in Figure S8 of the Supporting Information.

2.5. Chemicals. Potassium HAS and potassium propyl sulfate were synthesized according to established literature procedures,[42,43] which are summarized in the Supporting Information. Nuclear magnetic resonance (NMR) spectra, high-resolution mass spectra, and product ion scans of the synthesized OS are presented in Figures S9−S12 of the Supporting Information. Deionized water was obtained from a Millipore Synergy UV ultrapure water system. All other chemicals were obtained from commercial suppliers and used as received, as outlined in the Supporting Information.

3. RESULTS AND DISCUSSION

3.1. TiO_2-Catalyzed Production of HAS: Influence of Illumination Time and Catalyst Loading. Given the compositional complexity of natural mineral samples,[44] we first conducted studies of OS formation in the presence of commercial TiO_2. As shown in Figure 1, illumination of MACR in aqueous Na_2SO_4 in the presence of TiO_2 leads to the production of HAS, an OS not only identified in previous studies of sulfate radical-catalyzed OS formation from this precursor[17,27,28] but also commonly measured in ambient PM.[12,27,45]

Figure 1 shows that HAS production increases linearly with illumination time and monotonically but nonlinearly with increasing TiO_2 loadings; in the absence of TiO_2, HAS is not produced. Although plateaus in TiO_2-catalyzed photochemistry at elevated catalyst loadings are generally attributed to catalyst agglomeration and light-shielding effects,[46,47] these effects typically become important at higher loadings than those explored in these experiments. For example, even though we estimate no reduction in effective photon flux in our reactor in the presence of 0.25 mg mL^{-1} TiO_2 (using chemical actinometry of 2-nitrobenzaldehyde[38]; results not shown), we observed nonlinear HAS production at even lower catalyst loadings (e.g., HAS production at 0.1 mg mL^{-1} TiO_2 was only ~50% larger than at 0.01 mg mL^{-1}).

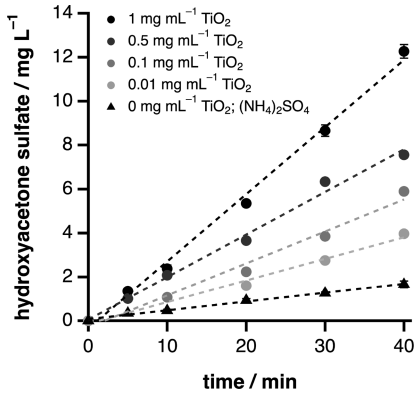

Figure 1. Time-dependent HAS production from MACR (10 mM) in illuminated suspensions of TiO_2 in aqueous Na_2SO_4 (1 M; adjusted to pH 5) or $(NH_4)_2SO_4$ (1 M) in the absence of TiO_2. For experiments at the highest TiO_2 loading, all TiO_2 loadings at 30 min, and in the presence of $(NH_4)_2SO_4$, data points represent the mean of three trials, with 1σ error bars; otherwise, data points show the results of one trial. The dashed lines are linear fits to the experimental data.

We attribute the nonlinearity in HAS production with respect to TiO_2 loadings to the TiO_2-catalyzed loss of HAS, which we would expect to adsorb to the TiO_2 surface more strongly than MACR as a result of favorable electrostatic interactions between TiO_2 and its anionic sulfate moiety.[32] Support for this interpretation is provided by a set of experiments (Figure S13 of the Supporting Information) showing rapid loss of HAS in the presence of 0.5 mg mL^{-1} TiO_2, only partial inhibition of this loss in the presence of MACR, and no HAS loss in the presence of TiO_2 under dark conditions. Because all of the experiments shown in Figure 1 were performed at the same MACR (10 mM) and sulfate (1 M) concentrations, we would expect competitive adsorption by both MACR and sulfate anion[33] to limit HAS loss most effectively at lower TiO_2 loadings.

3.2. TiO_2-Catalyzed Production of HAS: Sulfate Concentration Dependence and Cation Effects. As shown in Figure 2, TiO_2-catalyzed HAS production from MACR in aqueous Na_2SO_4 displays a nonlinear dependence upon sulfate anion concentration. These results are consistent with a surface reaction mechanism, in which HAS production

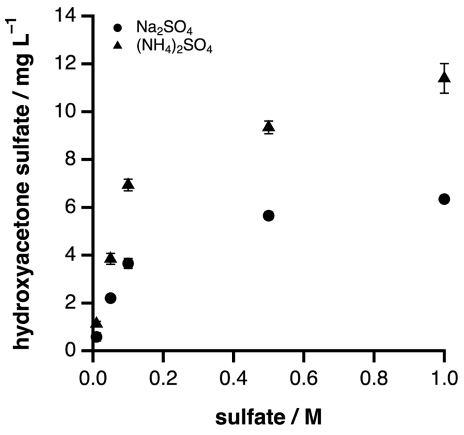

Figure 2. HAS production from MACR (10 mM) in illuminated (30 min) suspensions of TiO_2 (0.5 mg mL^{-1}) in aqueous Na_2SO_4 (1 M; adjusted to pH 5) or $(NH_4)_2SO_4$ (1 M). Each data point represents the mean of three trials, with 1σ error bars.

DOI: 10.1021/acsearthspacechem.8b00178
ACS Earth Space Chem. XXXX, XXX, XXX−XXX

at elevated sulfate anion concentrations is limited by the saturation of available surface sites for adsorption. In our proposed mechanism, sulfate adsorbs to the TiO_2 surface, where it undergoes one-electron oxidation,[33] and the resultant sulfate radical subsequently adds to MACR to yield HAS via the mechanism[27] shown in Scheme 1.

Scheme 1. Proposed Mechanism for Production of HAS (m/z 153) via Sulfate Radical Addition to MACR

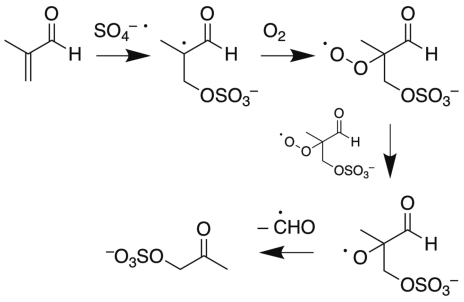

Sulfate radical can also be formed in bulk aqueous solution via the reaction of hydroxyl radical, produced here via TiO_2 photocatalysis,[48] with hydrogen sulfate anion ($k = 3.5 \times 10^5$ M^{-1} s^{-1}).[49] However, under our experimental conditions (i.e., pH 5, where [HSO_4^-] ~1 mM), the reaction of hydroxyl radical with MACR (10 mM; $k = 9.4 \times 10^9$ M^{-1} s^{-1})[50] would dominate at even the highest sulfate anion concentrations. Therefore, HAS production via this mechanism would be expected to increase linearly with increasing sulfate anion concentration, which is inconsistent with our results. In the absence of further data, we cannot exclude that the production of the hydroxyl radical itself exhibits a plateau at elevated sulfate anion concentrations. Quantification of hydroxyl and sulfate radical production *in situ* via the use of probe molecules[51] would provide further insight into the fundamental mechanism(s) underlying the observed results, but is beyond the scope of the current work.

Interestingly, Figure 2 shows that the TiO_2-catalyzed production of HAS is higher in aqueous $(NH_4)_2SO_4$ than in aqueous Na_2SO_4; in addition, as displayed in Figure 1, illumination of MACR in aqueous $(NH_4)_2SO_4$ leads to the production of modest quantities of HAS, even in the absence of TiO_2. This latter observation agrees with Noziere et al., who observed the formation of a range of OS upon illumination of MACR in concentrated aqueous $(NH_4)_2SO_4/Na_2SO_4$.[17] We suggest that all of these observations can be explained by a multistep process for the formation of additional sulfate radical, involving the production of light-absorbing SOA material by the reaction of ammonium with MACR,[52] the subsequent photolysis of this material, and the reaction of the hydroxyl radicals thus formed[53] with hydrogen sulfate anion to yield sulfate radicals. Because, as discussed above, the aqueous-phase reaction of hydroxyl radical with hydrogen sulfate anion is slow compared to its reaction with dissolved organics, sulfate radical production via this reaction would be expected to represent a minor reaction channel for photoproduced hydroxyl radical. Our observations of enhanced OS production in aqueous $(NH_4)_2SO_4$ therefore suggest that absolute hydroxyl radical production from photolysis of ammonium–MACR reaction products may be substantial. We are currently conducting *in situ* quantification of hydroxyl radical production[53] in this experimental system, which we anticipate will help to explain these observations.

3.3. TiO_2-Catalyzed Production of Additional OS Products: MACR Concentration Dependence and Cation Effects. To gain further insight into TiO_2-catalyzed OS formation, we also performed experiments as a function of MACR concentration (1–40 mM) in both aqueous Na_2SO_4 and $(NH_4)_2SO_4$. In both cases, the production of HAS does not increase with increasing MACR concentration (Figure S14 of the Supporting Information). In the context of our proposed mechanism for HAS production, this observation is consistent with the reaction being sulfate radical-limited over this MACR concentration range.

As shown in Figure 3, the production of several OS compounds with m/z 253 [liquid chromatography–tandem mass spectrometry (LC–MS/MS) chromatograms show multiple peaks; Figure S5 of the Supporting Information] increases with increasing MACR concentrations in both aqueous Na_2SO_4 and $(NH_4)_2SO_4$. In addition, the total m/z 253 signal increases linearly with illumination time (Figure S15 of the Supporting Information), which implies that it reflects contributions from first-generation products rather than products formed from further reaction of HAS. These results are consistent with previously proposed formation mechanisms for these species,[17,27] in which the alkyl radical produced via sulfate radical reaction with MACR reacts with an additional molecule of MACR to ultimately form a set of isomeric OS dimers with m/z 253 (Table 1). In addition, these results provide insight into a recent study by Wach et al.,[28] which did not report production of these dimeric OS from the solar irradiation of dilute (0.2 mM) MACR solutions containing potassium persulfate as sulfate radical precursor. Finally, we note with reference to Figure S15 of the Supporting Information that the production of the m/z 253 OS increases exponentially with TiO_2 loadings, with production at 1 mg mL^{-1} approximately 4 times larger than that at 0.5 mg mL^{-1}. In the context of previous work,[27] which has shown m/z 253 to be photolytically labile, we hypothesize that these observations reflect reductions in effective photon flux in our reactor at these elevated TiO_2 loadings. Further, they imply that, unlike HAS, the dimeric m/z 253 OS do not undergo substantial TiO_2-catalyzed loss, most likely as a result of their relatively

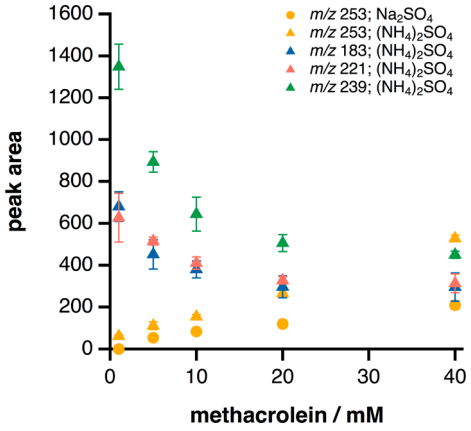

Figure 3. OS production from MACR in illuminated (30 min) suspensions of TiO_2 (0.5 mg mL^{-1}) in aqueous Na_2SO_4 (1 M; adjusted to pH 5) or $(NH_4)_2SO_4$ (1 M). Each data point represents the mean of three trials, with 1σ error bars.

DOI: 10.1021/acsearthspacechem.8b00178
ACS Earth Space Chem. XXXX, XXX, XXX–XXX

Table 1. Proposed Structures for the OS Observed in the Present Experiments

m/z $[M - H]^{-1}$	Proposed structure	References
153	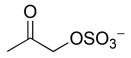	27,28
167	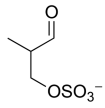	27
183*	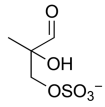	27,28
221*	unknown	27
239	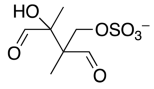	17
253*	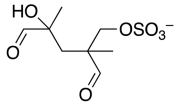	17,27

*OS for which LC−MS/MS chromatograms show evidence for multiple isomers.

more hydrophobic nature and resultant lower propensity to adsorb to the TiO_2 surface.

Interestingly, Figure 3 also shows that three additional OS with *m/z* 183, 221, and 239 are produced when $(NH_4)_2SO_4$ is used as the sulfate source; these OS, as well as the *m/z* 253 OS, are also produced in smaller quantities in the absence of TiO_2 (results not shown). Together, these results provide additional evidence for the importance of ammonium-mediated pathways in photochemical OS formation. All three of these OS have been previously reported in one or more laboratory studies of sulfate radical-mediated OS formation;[17,27,28] in addition, OS with *m/z* 183[27,42] and *m/z* 239[54,55] have been reported in ambient samples. The production of these OS decreases with increasing MACR concentrations, which suggests that the ammonium-mediated OS formation pathways discussed above are suppressed by competing reaction pathways at elevated MACR concentrations. Proposed structures for these additional OS are presented in Table 1.

3.4. Unexpectedly High OS Production in the Presence of Natural Mineral Samples. To assess the environmental relevance of the TiO_2-catalyzed OS formation pathway described in the previous sections, we also conducted experiments using natural anatase, ilmenite, and mica as well as road dust collected in Edmonton, Alberta. Interestingly, as shown in Figure 4, HAS concentrations resulting from illumination of MACR in aqueous Na_2SO_4 in the presence of these samples are the same order of magnitude as the HAS concentration in suspensions of commercial TiO_2. Because we would expect these samples to have lower inherent photoreactivity than TiO_2, these results are surprising.

As discussed in section 3.1, HAS undergoes rapid TiO_2-catalyzed photodegradation, even in the presence of MACR.

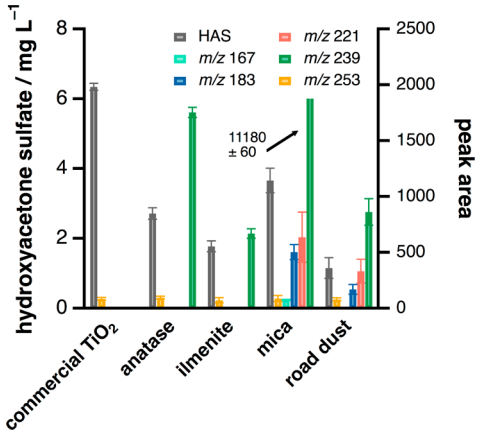

Figure 4. Production of HAS (mg L^{-1}; *m/z* 153) and other OS (peak area) from MACR (10 mM) in illuminated (30 min) suspensions of TiO_2 and natural mineral samples (0.5 mg mL^{-1}) in aqueous Na_2SO_4 (1 M; adjusted to pH 5). Each data point represents the mean of three trials, with 1σ error bars.

Although little is currently known regarding aerosol-phase OS loss pathways, these results complement those of two recent studies exploring the heterogeneous hydroxyl radical oxidation of sodium methyl sulfate[31] and 3-methyltetrol sulfate ester.[56] Because we would expect HAS loss to be influenced not only by MACR but also by competitive adsorption of sulfate at the surface of the samples employed in this study, a full understanding of HAS formation and loss kinetics in our experimental system would require experiments as a function of both MACR and sulfate concentrations for each sample type. Although these experiments are beyond the scope of the present study, our preliminary results suggest the need for further investigation of mineral-catalyzed OS loss.

Although the similarity in apparent HAS production between commercial TiO_2 and natural mineral samples may simply reflect efficient loss of HAS at the surface of TiO_2, as discussed above, we posit that it may also reflect the existence of additional OS production pathways in the presence of these more complex substrates. Support for this latter suggestion is provided by Figure 4, which shows production of a broader range of OS in the presence of mica and road dust than in the presence of commercial TiO_2. The OS produced in the highest quantity in these experiments is one with *m/z* 239, which is of interest because an OS with this mass-to-charge ratio has been reported in ambient PM, in some cases in large quantities.[15,54,55] In one study, Mutzel et al.[55] suggested that this OS arose via the interaction of gas-phase organic species with acidic PM; in another study, Brüggeman et al.[54] showed that formation of this OS also occurred under low-acidity PM conditions. Here, we provide evidence for a pathway for the formation of this OS that does not require acidic conditions.

3.5. Mineral-Catalyzed OS Production: Implications for Catalysis and Atmospheric Aerosol Composition. In a seminal study, Abdullah et al. reported that the TiO_2-catalyzed photooxidation of organic solutes was not fully inhibited in the presence of sulfate, even though this anion would be expected to competitively occupy surface oxidizing sites.[33] These authors attributed this observation to sulfate radical production at the TiO_2 surface and subsequent reaction of this species with the organic solutes studied. Our observations of HAS production from MACR in suspensions of TiO_2 in aqueous sulfate solution provide the first direct

DOI: 10.1021/acsearthspacechem.8b00178
ACS Earth Space Chem. XXXX, XXX, XXX−XXX

evidence in support of this hypothesis; in addition, they highlight the need for further mechanistic studies of the influence of inorganic anions on the product distribution resulting from TiO_2-catalyzed aqueous organic photochemistry.

More broadly and in an atmospheric context, our results also highlight the importance of mineral-mediated photochemistry for the aqueous-phase production of OS from unsaturated organic precursors. Although mineral dust is primarily emitted in remote arid regions,[57] it undergoes efficient long-range transport and can interact with potential organic OS precursors both during transport[58,59] and upon arrival in urban[60] and/or remote[61] receptor regions; in addition, dust is often internally mixed with sulfate.[62] In this context, our results represent an important first step toward understanding the photochemical sources of OS in dust-influenced regions.

■ ASSOCIATED CONTENT

Supporting Information

The Supporting Information is available free of charge on the ACS Publications website at DOI: 10.1021/acsearthspacechem.8b00178.

Additional sample characterization and experimental details, Figures S1−S15, and Tables S1−S3 (PDF)

■ AUTHOR INFORMATION

Corresponding Author

*Telephone: 780-492-6659. E-mail: sstyler@ualberta.ca.

ORCID

Mario Schmidt: 0000-0001-9134-8077
Maya Abou-Ghanem: 0000-0003-1417-8937
Anton O. Oliynyk: 0000-0003-0732-7340
Sarah A. Styler: 0000-0002-6078-9387

Notes

The authors declare no competing financial interest.

■ ACKNOWLEDGMENTS

The authors acknowledge the Department of Chemistry and the Faculty of Science at the University of Alberta for start-up funding, the Natural Sciences and Engineering Research Council of Canada (NSERC) for funding through the Discovery Grant program, the Canada Foundation for Innovation (CFI) for funding through the John R. Evans Leaders Fund, and the Alberta Ministry of Economic Development and Trade for funding through the Small Equipment Grants stream of the Research Capacity Program. The authors thank Khyati Gohil and Dr. Florence Williams for assistance with OS synthesis, Dr. Randy Whittal for assistance with LC−MS/MS analysis, Katie Nichols for assistance with mineral phase identification, and Ming Lyu for performing BET surface area measurements. The authors thank Vincent Bizon, Allan Chilton, Dirk Kelm, and Jason Dibbs for construction of the photochemical reactor employed in these experiments. The authors thank Wanda Goulden and Clarence Stuart at the City of Edmonton for facilitating winter street sweeping collection. The authors thank Faith Wierenga and Tania Gautam for assistance with preliminary experiments and Drs. D. James Donaldson, Manolis Romanias, and Frédéric Thévenet for useful discussions.

■ REFERENCES

(1) Choobari, O. A.; Zawar-Reza, P.; Sturman, A. The Global Distribution of Mineral Dust and Its Impacts on the Climate System: A Review. *Atmos. Res.* **2014**, *138*, 152−165.

(2) Shrivastava, M.; Cappa, C. D.; Fan, J.; Goldstein, A. H.; Guenther, A. B.; Jimenez, J. L.; Kuang, C.; Laskin, A.; Martin, S. T.; Ng, N. L.; Petaja, T.; Pierce, J. R.; Rasch, P. J.; Roldin, P.; Seinfeld, J. H.; Shilling, J.; Smith, J. N.; Thornton, J. A.; Volkamer, R.; Wang, J.; Worsnop, D. R.; Zaveri, R. A.; Zelenyuk, A.; Zhang, Q. Recent Advances in Understanding Secondary Organic Aerosol: Implications for Global Climate Forcing. *Rev. Geophys.* **2017**, *55* (2), 509−559.

(3) von Schneidemesser, E.; Monks, P. S.; Allan, J. D.; Bruhwiler, L.; Forster, P.; Fowler, D.; Lauer, A.; Morgan, W. T.; Paasonen, P.; Righi, M.; Sindelarova, K.; Sutton, M. A. Chemistry and the Linkages between Air Quality and Climate Change. *Chem. Rev.* **2015**, *115* (10), 3856−3897.

(4) Abbatt, J. P. D.; Lee, A. K. Y.; Thornton, J. A. Quantifying Trace Gas Uptake to Tropospheric Aerosol: Recent Advances and Remaining Challenges. *Chem. Soc. Rev.* **2012**, *41* (19), 6555−6581.

(5) Mazzoleni, L. R.; Saranjampour, P.; Dalbec, M. M.; Samburova, V.; Hallar, A. G.; Zielinska, B.; Lowenthal, D. H.; Kohl, S. Identification of Water-Soluble Organic Carbon in Non-Urban Aerosols Using Ultrahigh-Resolution FT-ICR Mass Spectrometry: Organic Anions. *Environ. Chem.* **2012**, *9* (3), 285−297.

(6) Schmitt-Kopplin, P.; Gelencsér, A.; Dabek-Zlotorzynska, E.; Kiss, G.; Hertkorn, N.; Harir, M.; Hong, Y.; Gebefügi, I. Analysis of the Unresolved Organic Fraction in Atmospheric Aerosols with Ultrahigh-Resolution Mass Spectrometry and Nuclear Magnetic Resonance Spectroscopy: Organosulfates As Photochemical Smog Constituents. *Anal. Chem.* **2010**, *82* (19), 8017−8026.

(7) Wozniak, A. S.; Bauer, J. E.; Sleighter, R. L.; Dickhut, R. M.; Hatcher, P. G. Technical Note: Molecular Characterization of Aerosol-Derived Water Soluble Organic Carbon Using Ultrahigh Resolution Electrospray Ionization Fourier Transform Ion Cyclotron Resonance Mass Spectrometry. *Atmos. Chem. Phys.* **2008**, *8* (17), 5099−5111.

(8) Zhang, J.; Jiang, B.; Wang, Z.; Liang, Y.; Zhang, Y.; Xu, C.; Shi, Q. Molecular Characterisation of Ambient Aerosols by Sequential Solvent Extractions and High-Resolution Mass Spectrometry. *Environ. Chem.* **2018**, *15* (3), 150−161.

(9) Willoughby, A. S.; Wozniak, A. S.; Hatcher, P. G. A Molecular-Level Approach for Characterizing Water-Insoluble Components of Ambient Organic Aerosol Particulates Using Ultrahigh-Resolution Mass Spectrometry. *Atmos. Chem. Phys.* **2014**, *14* (18), 10299−10314.

(10) Hansen, A. M. K.; Kristensen, K.; Nguyen, Q. T.; Zare, A.; Cozzi, F.; Nøjgaard, J. K.; Skov, H.; Brandt, J.; Christensen, J. H.; Ström, J.; Tunved, P.; Krejci, R.; Glasius, M. Organosulfates and Organic Acids in Arctic Aerosols: Speciation, Annual Variation and Concentration Levels. *Atmos. Chem. Phys.* **2014**, *14* (15), 7807−7823.

(11) Glasius, M.; Bering, M. S.; Yee, L. D.; de Sá, S. S.; Isaacman-VanWertz, G.; Wernis, R. A.; Barbosa, H. M. J.; Alexander, M. L.; Palm, B. B.; Hu, W.; Campuzano-Jost, P.; Day, D. A.; Jimenez, J. L.; Shrivastava, M.; Martin, S. T.; Goldstein, A. H. Organosulfates in Aerosols Downwind of an Urban Region in Central Amazon. *Environ. Sci.: Processes Impacts* **2018**, *20* (11), 1546−1558.

(12) Hettiyadura, A. P. S.; Jayarathne, T.; Baumann, K.; Goldstein, A. H.; de Gouw, J. A.; Koss, A.; Keutsch, F. N.; Skog, K.; Stone, E. A. Qualitative and Quantitative Analysis of Atmospheric Organosulfates in Centreville, Alabama. *Atmos. Chem. Phys.* **2017**, *17* (2), 1343−1359.

(13) Stone, E. A.; Yang, L.; Yu, L. E.; Rupakheti, M. Characterization of Organosulfates in Atmospheric Aerosols at Four Asian Locations. *Atmos. Environ.* **2012**, *47*, 323−329.

(14) Tolocka, M. P.; Turpin, B. Contribution of Organosulfur Compounds to Organic Aerosol Mass. *Environ. Sci. Technol.* **2012**, *46* (15), 7978−7983.

(15) Surratt, J. D.; Gómez-González, Y.; Chan, A. W. H.; Vermeylen, R.; Shahgholi, M.; Kleindienst, T. E.; Edney, E. O.; Offenberg, J. H.; Lewandowski, M.; Jaoui, M.; Maenhaut, W.; Claeys, M.; Flagan, R. C.;

DOI: 10.1021/acsearthspacechem.8b00178
ACS Earth Space Chem. XXXX, XXX, XXX−XXX

Seinfeld, J. H. Organosulfate Formation in Biogenic Secondary Organic Aerosol. *J. Phys. Chem. A* **2008**, *112* (36), 8345−8378.
(16) Lukács, H.; Gelencsér, A.; Hoffer, A.; Kiss, G.; Horváth, K.; Hartyáni, Z. Quantitative Assessment of Organosulfates in Size-Segregated Rural Fine Aerosol. *Atmos. Chem. Phys.* **2009**, *9* (1), 231−238.
(17) Nozière, B.; Ekström, S.; Alsberg, T.; Holmström, S. Radical-Initiated Formation of Organosulfates and Surfactants in Atmospheric Aerosols. *Geophys. Res. Lett.* **2010**, *37* (5), L05806.
(18) Hansen, A. M. K.; Hong, J.; Raatikainen, T.; Kristensen, K.; Ylisirniö, A.; Virtanen, A.; Petäjä, T.; Glasius, M.; Prisle, N. L. Hygroscopic Properties and Cloud Condensation Nuclei Activation of Limonene-Derived Organosulfates and Their Mixtures with Ammonium Sulfate. *Atmos. Chem. Phys.* **2015**, *15* (24), 14071−14089.
(19) Estillore, A. D.; Hettiyadura, A. P. S.; Qin, Z.; Leckrone, E.; Wombacher, B.; Humphry, T.; Stone, E. A.; Grassian, V. H. Water Uptake and Hygroscopic Growth of Organosulfate Aerosol. *Environ. Sci. Technol.* **2016**, *50* (8), 4259−4268.
(20) Surratt, J. D.; Kroll, J. H.; Kleindienst, T. E.; Edney, E. O.; Claeys, M.; Sorooshian, A.; Ng, N. L.; Offenberg, J. H.; Lewandowski, M.; Jaoui, M.; Flagan, R. C.; Seinfeld, J. H. Evidence for Organosulfates in Secondary Organic Aerosol. *Environ. Sci. Technol.* **2007**, *41* (2), 517−527.
(21) Darer, A. I.; Cole-Filipiak, N. C.; O'Connor, A. E.; Elrod, M. J. Formation and Stability of Atmospherically Relevant Isoprene-Derived Organosulfates and Organonitrates. *Environ. Sci. Technol.* **2011**, *45* (5), 1895−1902.
(22) Passananti, M.; Kong, L.; Shang, J.; Dupart, Y.; Perrier, S.; Chen, J.; Donaldson, D. J.; George, C. Organosulfate Formation through the Heterogeneous Reaction of Sulfur Dioxide with Unsaturated Fatty Acids and Long-Chain Alkenes. *Angew. Chem., Int. Ed.* **2016**, *55* (35), 10336−10339.
(23) Shang, J.; Passananti, M.; Dupart, Y.; Ciuraru, R.; Tinel, L.; Rossignol, S.; Perrier, S.; Zhu, T.; George, C. SO_2 Uptake on Oleic Acid: A New Formation Pathway of Organosulfur Compounds in the Atmosphere. *Environ. Sci. Technol. Lett.* **2016**, *3* (2), 67−72.
(24) Shen, X.; Wu, H.; Zhao, Y.; Huang, D.; Huang, L.; Chen, Z. Heterogeneous Reactions of Glyoxal on Mineral Particles: A New Avenue for Oligomers and Organosulfate Formation. *Atmos. Environ.* **2016**, *131*, 133−140.
(25) Huang, L.; Cochran, R. E.; Coddens, E. M.; Grassian, V. H. Formation of Organosulfur Compounds through Transition Metal Ion-Catalyzed Aqueous Phase Reactions. *Environ. Sci. Technol. Lett.* **2018**, *5* (6), 315−321.
(26) Perri, M. J.; Lim, Y. B.; Seitzinger, S. P.; Turpin, B. J. Organosulfates from Glycolaldehyde in Aqueous Aerosols and Clouds: Laboratory Studies. *Atmos. Environ.* **2010**, *44* (21), 2658−2664.
(27) Schindelka, J.; Iinuma, Y.; Hoffmann, D.; Herrmann, H. Sulfate Radical-Initiated Formation of Isoprene-Derived Organosulfates in Atmospheric Aerosols. *Faraday Discuss.* **2013**, *165*, 237−259.
(28) Wach, P.; Spólnik, G.; Rudziński, K. J.; Skotak, K.; Claeys, M.; Danikiewicz, W.; Szmigielski, R. Radical Oxidation of Methyl Vinyl Ketone and Methacrolein in Aqueous Droplets: Characterization of Organosulfates and Atmospheric Implications. *Chemosphere* **2019**, *214*, 1−9.
(29) Rudziński, K. J.; Gmachowski, L.; Kuznietsova, I. Reactions of Isoprene and Sulphoxy Radical-Anions − a Possible Source of Atmospheric Organosulphites and Organosulphates. *Atmos. Chem. Phys.* **2009**, *9* (6), 2129−2140.
(30) Ervens, B.; George, C.; Williams, J. E.; Buxton, G. V.; Salmon, G. A.; Bydder, M.; Wilkinson, F.; Dentener, F.; Mirabel, P.; Wolke, R.; Herrmann, H. CAPRAM 2.4 (MODAC Mechanism): An Extended and Condensed Tropospheric Aqueous Phase Mechanism and its Application. *J. Geophys. Res.* **2003**, *108* (D14), 4426.
(31) Kwong, K. C.; Chim, M. M.; Davies, J. F.; Wilson, K. R.; Chan, M. N. Importance of Sulfate Radical Anion Formation and Chemistry in Heterogeneous OH Oxidation of Sodium Methyl Sulfate, the Smallest Organosulfate. *Atmos. Chem. Phys.* **2018**, *18* (4), 2809−2820.
(32) Hoffmann, M. R.; Martin, S. T.; Choi, W.; Bahnemann, D. W. Environmental Applications of Semiconductor Photocatalysis. *Chem. Rev.* **1995**, *95* (1), 69−96.
(33) Abdullah, M.; Low, G. K.-C.; Matthews, R. W. Effects of Common Inorganic Anions on Rates of Photocatalytic Oxidation of Organic Carbon over Illuminated Titanium Dioxide. *J. Phys. Chem.* **1990**, *94* (17), 6820−6825.
(34) Fan, J.; Zhang, R. Atmospheric Oxidation Mechanism of Isoprene. *Environ. Chem.* **2004**, *1* (3), 140−149.
(35) Sindelarova, K.; Granier, C.; Bouarar, I.; Guenther, A.; Tilmes, S.; Stavrakou, T.; Müller, J.-F.; Kuhn, U.; Stefani, P.; Knorr, W. Global Data Set of Biogenic VOC Emissions Calculated by the MEGAN Model over the Last 30 Years. *Atmos. Chem. Phys.* **2014**, *14* (17), 9317−9341.
(36) van Pinxteren, D.; Plewka, A.; Hofmann, D.; Müller, K.; Kramberger, H.; Svrcina, B.; Bächmann, K.; Jaeschke, W.; Mertes, S.; Collett, J. L.; Herrmann, H. Schmücke Hill Cap Cloud and Valley Stations Aerosol Characterisation during FEBUKO (II): Organic Compounds. *Atmos. Environ.* **2005**, *39* (23-24), 4305−4320.
(37) Chen, H.; Nanayakkara, C. E.; Grassian, V. H. Titanium Dioxide Photocatalysis in Atmospheric Chemistry. *Chem. Rev.* **2012**, *112* (11), 5919−5948.
(38) Galbavy, E. S.; Ram, K.; Anastasio, C. 2-Nitrobenzaldehyde as a Chemical Actinometer for Solution and Ice Photochemistry. *J. Photochem. Photobiol., A* **2010**, *209* (2−3), 186−192.
(39) Anastasio, C.; McGregor, K. G. Chemistry of Fog Waters in California's Central Valley: 1. In Situ Photoformation of Hydroxyl Radical and Singlet Molecular Oxygen. *Atmos. Environ.* **2001**, *35* (6), 1079−1089.
(40) Faust, B. C.; Allen, J. M. Aqueous-Phase Photochemical Sources of Peroxyl Radicals and Singlet Molecular Oxygen in Clouds and Fog. *J. Geophys. Res.* **1992**, *97* (D12), 12913−12926.
(41) Warneck, P.; Williams, J. In *The Atmospheric Chemist's Companion*; Springer: Dordrecht, Netherlands, 2012; pp 271−314.
(42) Hettiyadura, A. P. S.; Stone, E. A.; Kundu, S.; Baker, Z.; Geddes, E.; Richards, K.; Humphry, T. Determination of Atmospheric Organosulfates Using HILIC Chromatography with MS Detection. *Atmos. Meas. Tech.* **2015**, *8* (6), 2347−2358.
(43) Nalesso, A.; Frison, G.; Favretto, D.; Maietti, S.; Ferrara, S. D. Synthesis and Characterization of Ethyl Sulfate and D_5-Ethyl Sulfate as Reference Substances for Applications in Clinical and Forensic Toxicology. *Rapid Commun. Mass Spectrom.* **2005**, *19* (23), 3612−3614.
(44) Cote, C. D.; Schneider, S. R.; Lyu, M.; Gao, S.; Gan, L.; Holod, A. J.; Chou, T. H. H.; Styler, S. A. Photochemical Production of Singlet Oxygen by Urban Road Dust. *Environ. Sci. Technol. Lett.* **2018**, *5* (2), 92−97.
(45) Huang, R.-J.; Cao, J.; Chen, Y.; Yang, L.; Shen, J.; You, Q.; Wang, K.; Lin, C.; Xu, W.; Gao, B.; Li, Y.; Chen, Q.; Hoffmann, T.; O'Dowd, C. D.; Bilde, M.; Glasius, M. Organosulfates in Atmospheric Aerosol: Synthesis and Quantitative Analysis of $PM_{2.5}$ from Xi'an, Northwestern China. *Atmos. Meas. Tech.* **2018**, *11* (6), 3447−3456.
(46) Ahmed, S.; Rasul, M. G.; Martens, W. N.; Brown, R.; Hashib, M. A. Heterogeneous Photocatalytic Degradation of Phenols in Wastewater: A Review on Current Status and Developments. *Desalination* **2010**, *261* (1), 3−18.
(47) Herrmann, J.-M. Heterogeneous Photocatalysis: Fundamentals and Applications to the Removal of Various Types of Aqueous Pollutants. *Catal. Today* **1999**, *53* (1), 115−129.
(48) Nosaka, Y.; Nosaka, A. Y. Generation and Detection of Reactive Oxygen Species in Photocatalysis. *Chem. Rev.* **2017**, *117* (17), 11302−11336.
(49) Tang, Y.; Thorn, R. P.; Mauldin, R. L.; Wine, P. H. Kinetics and Spectroscopy of the SO_4^- Radical in Aqueous Solution. *J. Photochem. Photobiol., A* **1988**, *44* (3), 243−258.
(50) Schöne, L.; Schindelka, J.; Szeremeta, E.; Schaefer, T.; Hoffmann, D.; Rudzinski, K. J.; Szmigielski, R.; Herrmann, H. Atmospheric Aqueous Phase Radical Chemistry of the Isoprene Oxidation Products Methacrolein, Methyl Vinyl Ketone, Methacrylic

DOI: 10.1021/acsearthspacechem.8b00178
ACS Earth Space Chem. XXXX, XXX, XXX−XXX

Acid and Acrylic Acid − Kinetics and Product Studies. *Phys. Chem. Chem. Phys.* **2014**, *16* (13), 6257−6272.
(51) Liang, C.; Su, H.-W. Identification of Sulfate and Hydroxyl Radicals in Thermally Activated Persulfate. *Ind. Eng. Chem. Res.* **2009**, *48* (11), 5558−5562.
(52) Li, Z.; Nizkorodov, S. A.; Chen, H.; Lu, X.; Yang, X.; Chen, J. Nitrogen-Containing Secondary Organic Aerosols Formation by Acrolein Reaction with Ammonia/Ammonium. *Atmos. Chem. Phys.* **2019**, *19* (2), 1343−1356.
(53) Badali, K. M.; Zhou, S.; Aljawhary, D.; Antiñolo, M.; Chen, W. J.; Lok, A.; Mungall, E.; Wong, J. P. S.; Zhao, R.; Abbatt, J. P. D. Formation of Hydroxyl Radicals from Photolysis of Secondary Organic Aerosol Material. *Atmos. Chem. Phys.* **2015**, *15* (14), 7831−7840.
(54) Brüggemann, M.; Poulain, L.; Held, A.; Stelzer, T.; Zuth, C.; Richters, S.; Mutzel, A.; van Pinxteren, D.; Iinuma, Y.; Katkevica, S.; Rabe, R.; Herrmann, H.; Hoffmann, T. Real-Time Detection of Highly Oxidized Organosulfates and BSOA Marker Compounds during the F-BEACh 2014 Field Study. *Atmos. Chem. Phys.* **2017**, *17* (2), 1453−1469.
(55) Mutzel, A.; Poulain, L.; Berndt, T.; Iinuma, Y.; Rodigast, M.; Böge, O.; Richters, S.; Spindler, G.; Sipilä, M.; Jokinen, T.; Kulmala, M.; Herrmann, H. Highly Oxidized Multifunctional Organic Compounds Observed in Tropospheric Particles: A Field and Laboratory Study. *Environ. Sci. Technol.* **2015**, *49* (13), 7754−7761.
(56) Lam, H. K.; Kwong, K. C.; Poon, H. Y.; Davies, J. F.; Zhang, Z.; Gold, A.; Surratt, J. D.; Chan, M. N. Heterogeneous OH Oxidation of Isoprene Epoxydiol-Derived Organosulfates: Kinetics, Chemistry and Formation of Inorganic Sulfate. *Atmos. Chem. Phys. Discuss.* **2018**, 1−20 in review .
(57) Tanaka, T. Y.; Chiba, M. A Numerical Study of the Contributions of Dust Source Regions to the Global Dust Budget. *Glob. Planet. Change* **2006**, *52* (1), 88−104.
(58) Ansmann, A.; Baars, H.; Tesche, M.; Müller, D.; Althausen, D.; Engelmann, R.; Pauliquevis, T.; Artaxo, P. Dust and Smoke Transport from Africa to South America: Lidar Profiling over Cape Verde and the Amazon Rainforest. *Geophys. Res. Lett.* **2009**, *36* (11), L11802.
(59) Falkovich, A. H.; Schkolnik, G.; Ganor, E.; Rudich, Y. Adsorption of Organic Compounds Pertinent to Urban Environments onto Mineral Dust Particles. *J. Geophys. Res.* **2004**, *109* (D2), D02208.
(60) Shao, M.; Lu, S.; Liu, Y.; Xie, X.; Chang, C.; Huang, S.; Chen, Z. Volatile Organic Compounds Measured in Summer in Beijing and Their Role in Ground-level Ozone Formation. *J. Geophys. Res.* **2009**, *114*, D00G06.
(61) Liu, Y.; Brito, J.; Dorris, M. R.; Rivera-Rios, J. C.; Seco, R.; Bates, K. H.; Artaxo, P.; Duvoisin, S.; Keutsch, F. N.; Kim, S.; Goldstein, A. H.; Guenther, A. B.; Manzi, A. O.; Souza, R. A. F.; Springston, S. R.; Watson, T. B.; McKinney, K. A.; Martin, S. T. Isoprene Photochemistry over the Amazon Rainforest. *Proc. Natl. Acad. Sci. U. S. A.* **2016**, *113* (22), 6125−6130.
(62) Sullivan, R. C.; Guazzotti, S. A.; Sodeman, D. A.; Prather, K. A. Direct Observations of the Atmospheric Processing of Asian Mineral Dust. *Atmos. Chem. Phys.* **2007**, *7* (5), 1213−1236.

DOI: 10.1021/acsearthspacechem.8b00178
ACS Earth Space Chem. XXXX, XXX, XXX−XXX